


## Dynamics of entangled domain walls in the PXP model under driving: Crossover from prethermalization to localization

Guanhua Chen <sup>1</sup>, Weijie Huang <sup>1</sup>, and Yao Yao <sup>1,2,\*</sup>

<sup>1</sup>*Department of Physics, South China University of Technology, Guangzhou 510640, China*

<sup>2</sup>*State Key Laboratory of Luminescent Materials and Devices, South China University of Technology, Guangzhou 510640, China*

 (Received 5 July 2022; revised 10 October 2022; accepted 8 November 2022; published 16 November 2022)

Based on the PXP model adapted for Rydberg-blockaded chains, we investigate the dynamics of topological domain walls between different quantum many-body scar states of  $\mathbb{Z}_2$  symmetry. It is found that the domain walls not only possess oscillating features of scars but also manifest longstanding bipartite entanglement with exactly unchanged flip-flop phase difference, suggesting their potential as a quantum information resource. A periodically driven field is exerted and the high-frequency drive gives rise to a crossover from prethermalization to Floquet localization. In order to investigate the stability of domain walls acting as information carriers, we further simulate the collision between them and find negligible influence on each other. Subsequently, the quench dynamics with domain walls reveals exotic physics and applicable potentials of nonthermalized scar states.

DOI: [10.1103/PhysRevB.106.174302](https://doi.org/10.1103/PhysRevB.106.174302)

### I. INTRODUCTION

The eigenstate thermalization hypothesis (ETH) governs most isolated quantum many-body systems [1–3]. According to ETH, systems in an instable state will rapidly lose their initial memories and become ergodic, and expectation values of any local observable can be then calculated by the canonical ensemble. It is thus quite interesting whether ETH can be violated or at least slowed down, so that quantum coherence can be alive long term. Many-body localization (MBL) serves as a general mechanism for the breaking of thermalization [4–7]. Alternatively, there are some many-body systems that are neither thermalized nor completely nonthermalized [8,9]. For instance, a special coherent oscillation has been observed in an experiment of the Rydberg atoms chain [10]. Such partially nonthermalized phenomenon is called a quantum many-body scar (QMBS) [11]. QMBS refers to those eigenstates that possess large overlap with initial states and do not strictly obey ETH, so it is clear that the emergence of QMBS strongly depends on the initial states [11–13].

In the experiment of Rydberg atoms, the prohibition of adjacent excitation in the chain is called the Rydberg blockade [14], which activates the mechanism of weak ergodicity breaking. The PXP model, an abstract and effective model derived from the transverse Ising model, was then proposed to describe this novel kind of blockade [12]. During the past several years, extensive and interdisciplinary physical subjects have been discussed in the framework of the PXP model, including the Ising quantum phase transition [15], time-crystalline order [16], and moderately disordered quantum simulators [17]. In spite of an extremely simple form, the PXP model preserves many profound features. Given some intuitively designed initial states, such as the so-called  $\mathbb{Z}_2$  and

$\mathbb{Z}_3$  states, the oscillations of some local observables persist over a long time and the quantum fidelity even shows periodic revivals [12].  $\mathbb{Z}_2$  states, e.g., refer to two degenerate configurations of alternating ground and Rydberg states of Rydberg atoms, which are also called charge density wave or Néel states.

There must emerge a topological domain wall (DW) between the two degenerate configurations labeled by  $|\mathbb{Z}_2\rangle$  and  $|\mathbb{Z}'_2\rangle$ . Different from those DWs introduced by Iadecola and Schecter [18], which is the domain between a single ground and Rydberg state in a spin-1/2 chain, here the DW is a topological charge similar to the soliton between two ground-state configurations of trans-polyacetylene described by the Su-Schrieffer-Heeger (SSH) model [19]. As elementary excitations, the vortex and magnetic skyrmion are also DW structures with exotic topological properties, especially the Néel skyrmion found in a ferromagnet and heavy-metal bilayer, which has 2D topological domain wall similar to our topological charge [20–22]. DW is even believed to emerge in high- $T_c$  superconductors with stripe phases [23]. In all these cases, the DWs are regarded as stable quasiparticles that can be utilized as a resource of information carriers in quantum computations [24,25]. We are then strongly motivated by the question of whether the DW in the PXP model is also stable and preserves longstanding quantum coherence.

In this work, we focus on the dynamics of single and double DWs among  $\mathbb{Z}_2$  states. In the single-DW case, we analyze the dissociation and quantum diffusion of the DW and show profound features of coherence and entanglement, different from that in the normal PXP model, which may help us further comprehend the ergodicity-breaking mechanism of QMBS. Via introducing a time-dependent phase difference between even and odd sites, we establish a Floquet system based on the PXP model. With low driven frequency, the system is found to be in a regime between thermalization and nonthermalization, which is so-called prethermalization

\*yaoyao2016@scut.edu.cn

[8], while with high enough driven frequency, the system enters into a disorder-free localized regime which is called DW localization. A similar transition occurred in the quantum link model (QLM) to study the gauge theories as well [26]. Double DWs and their collision are also investigated, pointing out the potential for being the quantum information carriers.

The remainder of this paper is organized as follows. In Sec. II we briefly review the PXP model and introduce the modified formulation with the forward-scattering approximation (FSA) [11]. We define an observable named  $\mathbb{Z}_2$  inhomogeneity to describe the explicit configuration of DW and the relevant diffusion process. In Sec. III, via the dynamic evolution, we investigate the PXP model with DWs. By adding a periodically driven field, the crossover between prethermalization and DW localization is observed. The system with a double DW is explored as well. Concluding remarks and outlook are presented in Sec. IV.

## II. MODEL

The original PXP model for describing the Rydberg blockade can be established as follows. As in the normal treatment that the blockade radius is solely one lattice spacing, so in a one-dimensional chain, a single atom is allowed to be in the Rydberg state only if its two nearest-neighbor atoms are simultaneously in the ground state [11,12]. We then set  $|0\rangle$  and  $|1\rangle$  to be the ground state and the excited Rydberg state, respectively. The two  $\mathbb{Z}_2$  states, i.e., charge density wave states, can be written as  $|\mathbb{Z}_2\rangle = |1010\dots\rangle$  and  $|\mathbb{Z}'_2\rangle = |0101\dots\rangle$ . The Rydberg blockade can be thus described by the model Hamiltonian

$$H_{\text{PXP}} = \sum_{i=1}^L P_{i-1} X_i P_{i+1}, \quad (1)$$

where  $X_i, Z_i$  are the usual Pauli operators on the  $i$ th site and  $P_i = (1 - Z_i)/2 = |0\rangle\langle 0|_i$  is the ground state projector. Throughout this paper, we assume the open boundary condition (OBC) and the boundary terms take the form  $X_1 P_2$  and  $P_{L-1} X_L$ , respectively. As we merely calculate the dynamics before DWs touch the ends of the chain, the boundary conditions are not important.

As observed in the experiment of Rydberg atoms, while quenching from  $|\mathbb{Z}_2\rangle$ , the system manifests a coherent and persistent oscillation [10]. Relevant numerical calculations of entanglement entropy and correlation function on the basis of the PXP model rebuilt the same oscillation frequency as measured in experiment. This oscillation survives in  $|\mathbb{Z}_3\rangle$  but vanishes for  $|\mathbb{Z}_4\rangle$  [11]. The survival of long-term oscillation is justified as prethermalization sensitive to the initial density of Rydberg states, just like that in the spin-glass model [27].

Furthermore, FSA was introduced as an approximation method in calculating the PXP model [11,12]. The Hamiltonian (1) is divided into two parts, namely  $H_{\text{PXP}} = H_+ + H_-$ , where the forward and backward propagators are defined as

$$H_{\pm} = \sum_{i \in \text{even}} P_{i-1} \sigma_i^{\pm} P_{i+1} + \sum_{i \in \text{odd}} P_{i-1} \sigma_i^{\mp} P_{i+1}, \quad (2)$$

with  $\sigma_i^+ = |1\rangle\langle 0|_i$  and  $\sigma_i^- = |0\rangle\langle 1|_i$ . When the initial state is  $|\mathbb{Z}_2\rangle$ , the  $H_+$  always increases the Hamming distance while  $H_-$  decreases it, with the Hamming distance defined as the minimum number of spin flips required from any given state to the  $|\mathbb{Z}_2\rangle$  [11,12]. By calculating the overlap between the eigenstates of Hamiltonian (1) and  $|\mathbb{Z}_2\rangle$ , FSA gives a result in good agreement with exact results [11].

In order to study the time crystals in the MBL phase, one normally has to split a period of time evolution into at least two sessions dominated by different Hamiltonians [28,29]. Here in this work, we consider another approach by noticing that  $H_+$  is nothing but the annihilator of  $|\mathbb{Z}'_2\rangle$ , and accordingly  $H_-$  annihilates  $|\mathbb{Z}_2\rangle$ . Similar to that in the gauge theory of electrons in the SSH model [30], we try to make a phase difference between these two degenerate states, instead of making two sessions of the Hamiltonian. Without loss of generality, we rewrite Hamiltonian (1) to be

$$H = e^{i\gamma t} H_+ + e^{-i\gamma t} H_-, \quad (3)$$

by adding a time-dependent phase difference between  $H_+$  and  $H_-$  with a period of  $2\pi/\gamma$ , which is equal to discriminating the even and odd sites.

Considering the PXP model was proposed to describe the Rydberg atom chain, it is of course not difficult to experimentally realize this phase difference by just adding a space-dependent phase modulated microwave as the driven field. In lattice gauge theories (LGTs), by mapping between Rydberg atoms and spin-1/2 QLM, a position-dependent  $\theta$ -angle term leads to confinement of particle-antiparticle pairs, which can be realized by an ac Stark shift or a detuning on the transition between ground and Rydberg states [26].

In order to investigate the dynamics of DW, the initial state is no longer the usual  $|\mathbb{Z}_2\rangle$ . In the single-DW case, e.g., the chain is divided into two parts: the left half is in  $|\mathbb{Z}_2\rangle$  and the right half in  $|\mathbb{Z}'_2\rangle$ . As a result, there is an interface between the two parts which can be represented as  $|\dots 1010:0101\dots\rangle$ , with  $:$  denoting the DW.

Different from other topological charges with stable shape, the DW in our model possesses the oscillating feature of QMBS, so we have to explicitly define a featured quantity to clearly observe the position and motion of this DW. It is intuitive to define the staggered difference between  $\langle Z_i \rangle$  of nearest sites, like that in the antiferromagnetic chain. Here, however, we have two configurations  $|\mathbb{Z}_2\rangle$  and  $|\mathbb{Z}'_2\rangle$ , so this normal definition will make the patterns shaky. Alternatively, we notice that there is a spatial inversion symmetry between the two halves of the chain; that is, the even and odd sites are exactly symmetric by spatial inversion during the evolution. We can then define a staggered difference between odd sites only, which we call  $\mathbb{Z}_2$  inhomogeneity. Namely, the definition writes

$$\Delta_k = \langle Z_{2k-1} \rangle - \langle Z_{2k+1} \rangle. \quad (4)$$

For both  $\mathbb{Z}_2$  configurations, this  $\mathbb{Z}_2$  inhomogeneity remains zero except for some unimportant boundary effects. It is

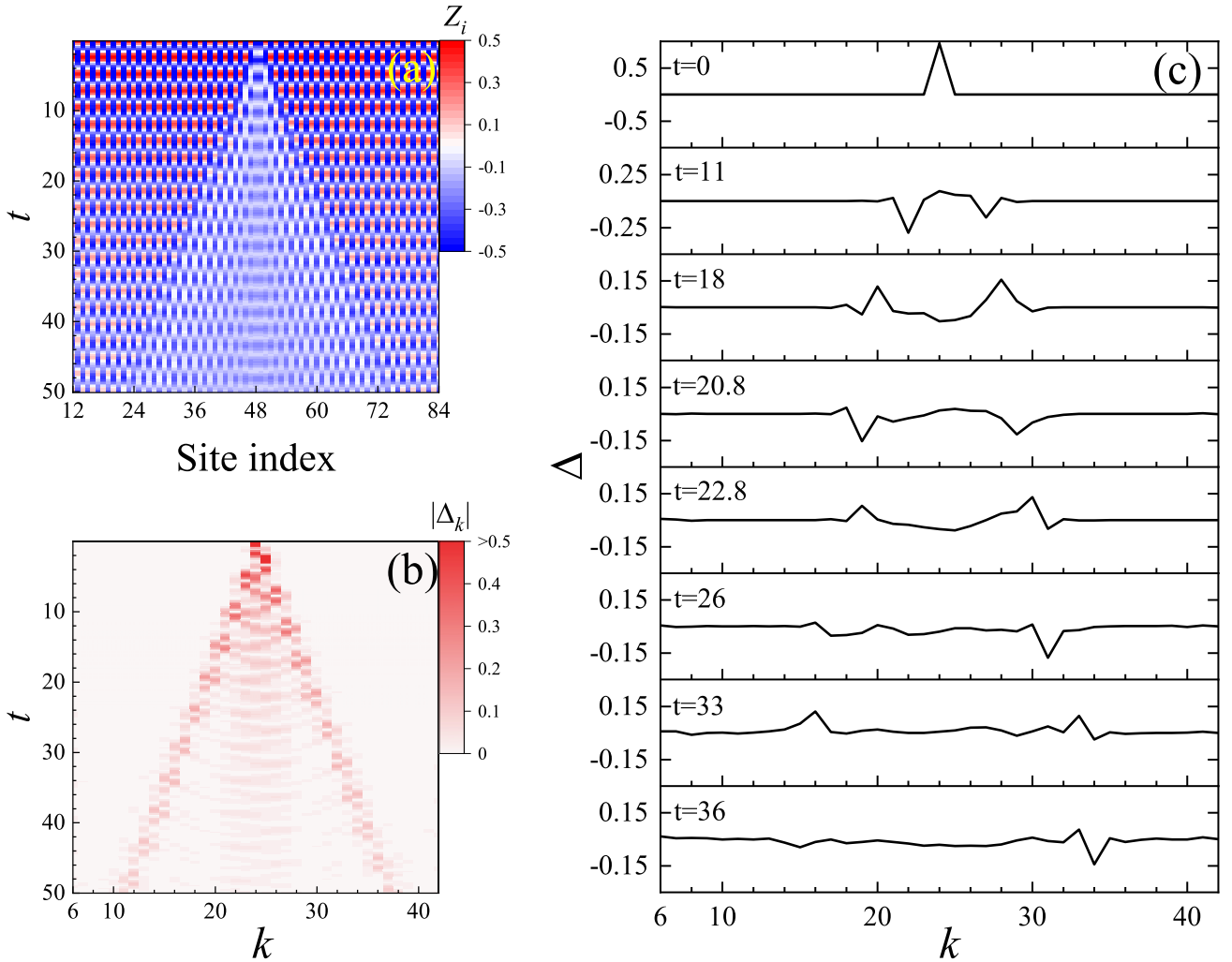


FIG. 1. Simulated process of single-DW dissociation and diffusion in PXP model for  $L = 96$  sites with OBC. The boundaries are not important, so the 12 sites close to each boundary are not shown. (a) Original observable  $\langle Z_i \rangle$  up to time  $t \sim 50$ . DW begins to diffuse from the middle of the chain. The amplitude of DW fluctuates between 0.5 and  $-0.5$  periodically. (b) The corresponding absolute value of  $\mathbb{Z}_2$  inhomogeneity  $|\Delta_k|$ . DW of (a) and (b) have the same envelop lines. But different from  $\langle Z_i \rangle$ , an oscillation like a pendulum between two generated DWs is observed. (c) The  $\mathbb{Z}_2$  inhomogeneity  $\Delta_k$  at eight typical time points. In the beginning, there is only one nonvanishing point, namely  $\Delta_{24} = 1$ . As time evolves, the DW is dissociated into two DWs and both of them spread out to the ends of the chain. It is also found that two peaks of dissociated DWs continuously flip and flop.

nonvanishing only when there is a DW in the chain. Taking an 8-site state  $|10100101\rangle$  for instance, only  $\Delta_2 = 1$  and others are vanishing, i.e.,  $\Delta_1 = \Delta_3 = \Delta_4 = 0$ , implying this newly defined inhomogeneity can be used to effectively describe the bipartition state DW.

### III. RESULTS

In the following, we numerically calculate the dynamical evolution of the system size  $L = 96$  for observing these DWs by time-evolving block decimation [31,32]. The computational accuracy depends on the maximal bond dimension of the resulting matrix product state. The PXP model needs more computational expense due to the lack of symmetry and 3-site Hamiltonian. Hence we choose OBC and moderate truncation dimension (maximum dimension  $\sim 70$ ) based on the trade-off between the accuracy and efficiency. Two initial states are

considered. The first is a single DW in the chain and the second goes to two DWs initially.

#### A. Entangled domain walls

We first analyze the dynamical evolution of a single initial DW in the chain with  $\gamma = 0$ , i.e., the normal PXP model. The initial DW is set at the center of the chain between  $i = 48$  and 49. In Fig. 1, we show the diffusion of DW up to  $t = 50$  in three ways. The first is the diffusion process of  $\langle Z_i \rangle$  displayed in Fig. 1(a). One can see that from the middle point of the chain the DW starts to dissociate and diffuse linearly with time. For pure  $|\mathbb{Z}_2\rangle$  or  $|\mathbb{Z}'_2\rangle$  initial state,  $\langle Z_i \rangle$  of each site has a persistent oscillation, which is the property of QMBS [12]. The DW in the chain is like a defect that breaks the perfect translational symmetry of the system. We further find that  $|\sum_{i=1}^L Z_i|$  is decreasing due to the diffusion, corresponding

to lighter and lighter pattern in the figure. This is because some  $|010\rangle$  state will become  $|000\rangle$  due to the PXP operations. We can also observe this situation for  $\mathbb{Z}_2$  inhomogeneity displayed in Fig. 1(b); that is, the red pattern becomes lighter while diffusing. These indicate that the amplitude of DW decays slowly and the system will subsequently thermalize which is nothing but the prethermalization of QMBS. Figure 1(c) shows the evolution of  $\Delta_k$  at eight typical time points. The first peak appearing at  $k = 24$  figures out the initial position of DW. Then, the DW dissociates into two that roughly preserve the line shape of wave packets and move toward two ends of the chain.

The most interesting point turns out to be that there is a pendulum-like oscillation between two generated DWs which can only be observed by  $\mathbb{Z}_2$  inhomogeneity. This implies that while almost keeping the shape of wave packets after dissociation of the original DW, the two generated DWs seem to keep quantum-mechanically communicating with each other. Just like we spatially separate an Einstein-Podolsky-Rosen pair that will preserve quantum entanglement [33], one would then intuitively ask if the two DWs are persistently entangled. Or equivalently, we want to know if the two DWs are in some sense like a singlet spin pair, in which if one spin is up, the other is down.

To this end, we have to divide the chain into bipartition systems and treat the data of inhomogeneity to be smoother. We then first calculate the velocity  $v$  of the two DWs by the peak values at each time point. From Fig. 1(b), we can obtain  $v \simeq 0.26$ . Next, we define two envelope functions which are time-dependent and normalized Gaussians:

$$f_{\pm}(t, k) = g_{\pm}(t) e^{-(k-k_0 \pm vt)^2}, \quad (5)$$

where  $g_{\pm}$  are the normalization coefficients and  $k_0$  is the initial position of DW. These two Gaussians are peaked at  $k = k_0 \pm vt$  so that we can make the left and right DWs individually outstanding. Finally, we define  $\Delta_{\pm}$  to signify the DWs as

$$\Delta_{\pm}(t) = \sum_k f_{\pm}(t, k) |\Delta_k|. \quad (6)$$

Figure 2 displays the results of  $\Delta_{\pm}$ , from which we can observe a very significant result. That is, the oscillations of two DWs after the first two periods are within exactly opposite phase, as indicated by the blue and purple lines. This exotic flip-flop effect of two DWs with unchanged phase difference well agrees with expectations in terms of QMBS, so it turns out to be the first significant result of this work. It is clearly exhibited that the two generated DWs after dissociation from the initial single DW preserve the phase coherence even if their spatial distance has become sufficiently long. More importantly, different from the soliton in SSH model which does not oscillate at all [30], the oscillations of DWs here can be controlled by external driven field, suggesting they can be potential candidates as resources of quantum information processing.

More straightforward quantities are obviously the correlation function and entanglement entropy. Figure 3(a) shows the evolution of correlation function  $\langle Z_i Z_{i+1} \rangle$  averaging on all  $i$ . An almost persistent oscillation is observed, just like the quench from the Néel state in the  $\langle Z_i Z_{i+1} \rangle$  decay process

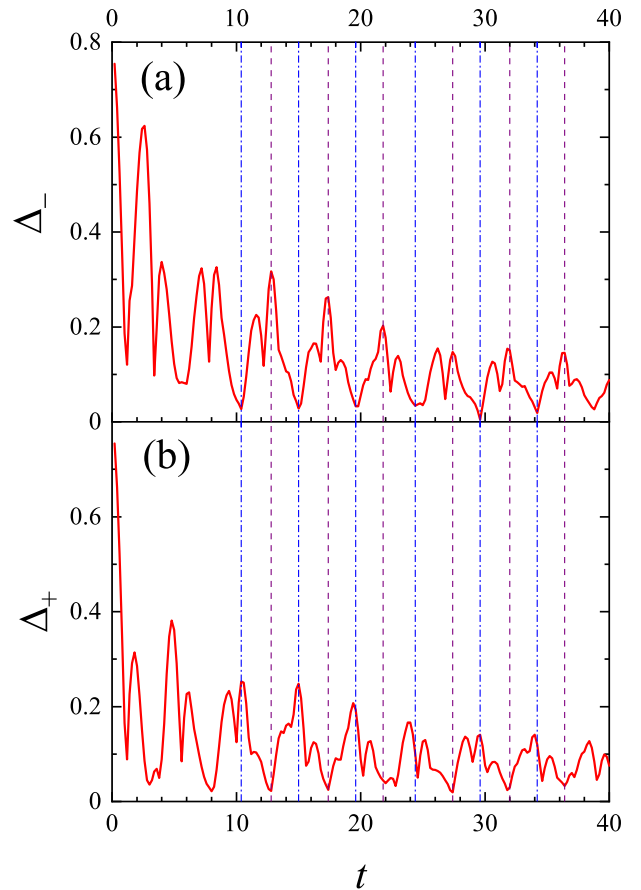


FIG. 2. Using  $\Delta_k$  and Gaussian envelop functions  $f_{\pm}(t, k)$  to obtain (a)  $\Delta_{-}$  and (b)  $\Delta_{+}$ , which exhibit the evolution of the two generated DWs. The corresponding  $\Delta_k$  are from Fig. 1 for  $t \sim 40$ . Vertical blue (purple) lines label the time point of the valleys (peaks) of  $\Delta_{-}$  and opposites of  $\Delta_{+}$ . It is shown that the two DWs persistently possess fixed phase differences.

[11]. Up to  $t = 50$ , the oscillation is not damped implying the quantum coherence is preserved long term. The oscillation period is the same with that of  $\Delta_k$  shown in Fig. 1.

Moreover, we calculate the von Neumann entanglement entropy  $S$  shown in Fig. 3(b), which is defined as  $S = -\text{Tr}(\rho \ln \rho)$  with  $\rho$  being the reduced density matrix for the left half of the chain. The long-time evolution of the entropy is just like that in the normal PXP model which manifests an oscillation and reaches maximum while quantum thermalizing. An interesting finding is that there is a significant drop at  $t = 3$ . Compared with later subtle variation about 0.1, this drop is more than 0.4. To explain this phenomenon, we can image the DW as a single particle on the initial stage and then it dissociates into two particles. The sudden spatial separation between two particles leads to the lift of initial degeneracy. In terms of the Holevo asymmetry measure, the asymmetry of the system decreases [34,35]. As a result, the entanglement between the two states declines abruptly at around  $t = 3$ . Afterward, as the system continues evolving, two particles leave away from each other and become separate substances. The entanglement of them is however preserved making each half of the chain into a completely mixed state, and the entropy

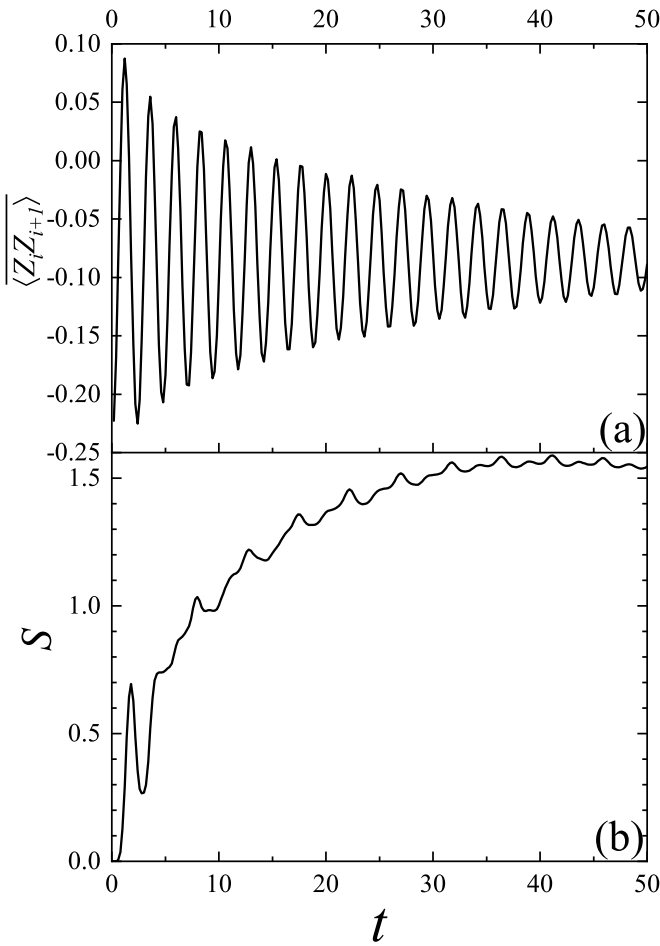


FIG. 3. Dynamics of PXP model with single-DW for  $t \sim 40$ . (a) Averaged local spin correlation function  $\langle Z_i Z_{i+1} \rangle$ . Coherent oscillation is damped very slowly figuring out the feature of prethermalization. (b) Bipartition entanglement entropy  $S$  between two halves of the chain. It is worth noting that there is a sudden drop at around  $t = 3$ .

of the left half is then decided by ergodicity of the canonical ensemble, which leads to subsequent entropy increase.

**B. Localization**

It is intriguing to consider whether we can manipulate the diffusion of DW, so we perform the simulations for finite  $\gamma > 0$  cases. Figure 4 shows the evolution of  $|\Delta_k|$  with  $\gamma = 0.5$ ,  $\gamma = 1$ , and  $\gamma = 4$ , respectively. These three values of  $\gamma$  result in completely different behaviors of Floquet character, changing from weak breakdown of ergodicity to localization. The first two cases, Figs. 4(a) and 4(b), display obscure dispersive patterns, while for  $\gamma = 4$  shown in Fig. 4(c), the DW completely stays in the middle of the chain without any dissociation. This localization of DW implies the initial memory of system remains for a sufficiently long time duration and thus the ETH is perfectly violated. We then conclude here that the gaugelike phase  $\gamma$  indeed induces the localization in the system of QMBS as expected.

One may be wondering whether this localization has properties of MBL. Namely, the periodically driven field  $e^{\pm i\gamma t}$

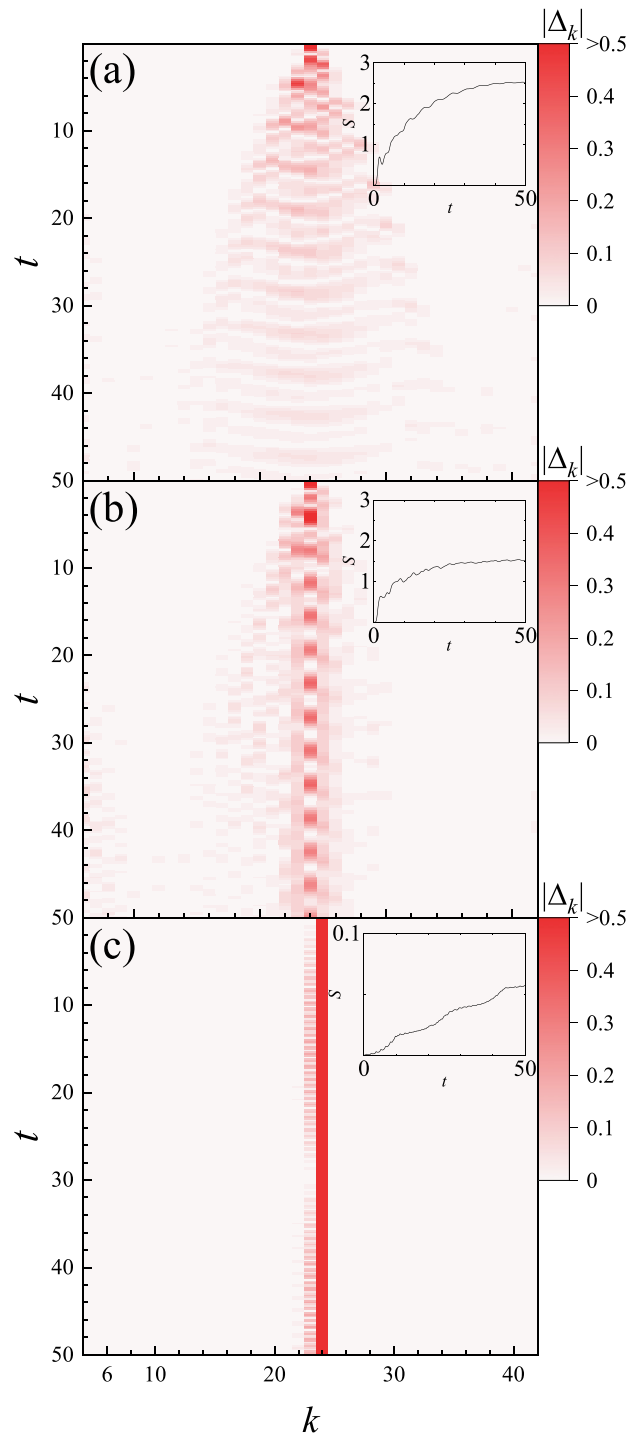


FIG. 4. Absolute value of  $\mathbb{Z}_2$  inhomogeneity  $|\Delta_k|$  with (a)  $\gamma = 0.5$ , (b)  $\gamma = 1$ , (c)  $\gamma = 4$ . As  $\gamma$  increases, the diffusion of DW becomes slower and slower. When  $\gamma = 4$ , the DW is localized at the center of the chain. Insets show the von Neumann entanglement entropy. From  $\gamma = 0.5$  to  $\gamma = 4$ , the value and increase rate of entropy get smaller.

may give rise to a transition from prethermalization to DW localization. In the inset of Fig. 4, we show the relevant von Neumann entanglement entropy of the left half of the chain. It is clear that with increasing  $\gamma$ , the magnitude of entanglement entropy decreases by around two orders. More importantly,



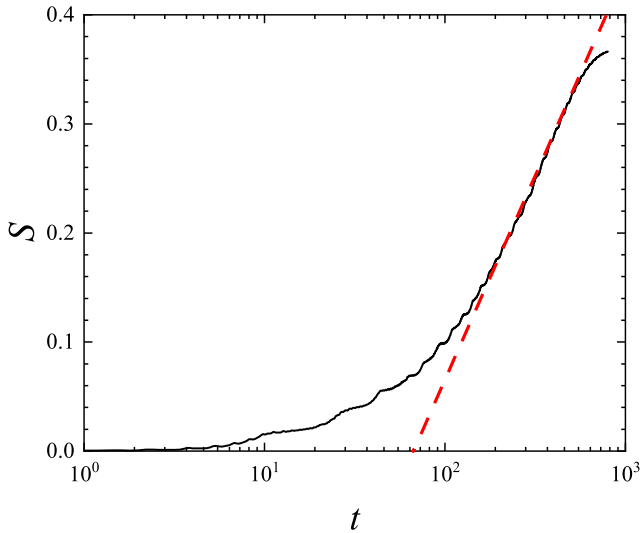


FIG. 5. Evolution of entanglement entropy  $S$  up to  $t \sim 800$  for the left half of the chain with  $\gamma = 4$ . The horizontal axis is in logarithmic scale, and the red dashed line represents a fitting. The subsequent deviation of logarithmic relation is due to the finite-size effect.

for small  $\gamma$  the entropy saturates very quickly, but for large  $\gamma$  it keeps increasing for a long time.

In order to see the line shape of the entanglement entropy at longer time duration, Fig. 5 displays the evolution of entropy for  $\gamma = 4$  up to  $t = 800$ . It is found that, after  $t = 100$ , the dependence of entropy on time becomes nearly logarithmic. At longer time, the entropy will be saturated due to the finite-size effect. It is well known that [36–38] the entropy continuously grows logarithmically in the MBL phase due to the Lieb-Robinson velocity of information communication between local integrals of motion. This suggests it is the quantum correlation between  $|\mathbb{Z}_2\rangle$  and  $|\mathbb{Z}'_2\rangle$  on opposite sides of the localized DW, due to the periodic external driven field.

To get insight into the role of  $\gamma$ , the evolution of entanglement entropy with  $\gamma$  being from 0 to 4 is shown in Fig. 6(a). The unusual drop appearing at  $t = 3$  discussed above becomes smoother as  $\gamma$  increases and disappears at around  $\gamma = 0.8$ . More remarkably, we can clearly see a significantly high entropy region from  $\gamma = 0$  to  $\gamma = 1$ . That is, as  $\gamma$  increases,  $S$  grows at first and then falls down. The entropies at several time points are averaged and shown in Fig. 6(b). For  $t = 50$ , entropy is kept stabilized and the maximum at  $\gamma = 0.6$  reveals a crossover between prethermalization and DW localization.

We then analyze  $H_{\pm}$  in Eq. (2) in greater detail. For mixed initial state,  $H_+$  solely acts on the part of  $|\mathbb{Z}_2\rangle$ , because  $H_+$  annihilates the whole  $|\mathbb{Z}'_2\rangle$ . For example, with a four-site  $|\mathbb{Z}_2\rangle$  state, the map of  $H_+$  writes

$$|1010\rangle \rightarrow |0010\rangle + |1000\rangle. \quad (7)$$

Conversely,  $H_-$  annihilates  $|\mathbb{Z}_2\rangle$  so the map is

$$|0101\rangle \rightarrow |0001\rangle + |0100\rangle. \quad (8)$$

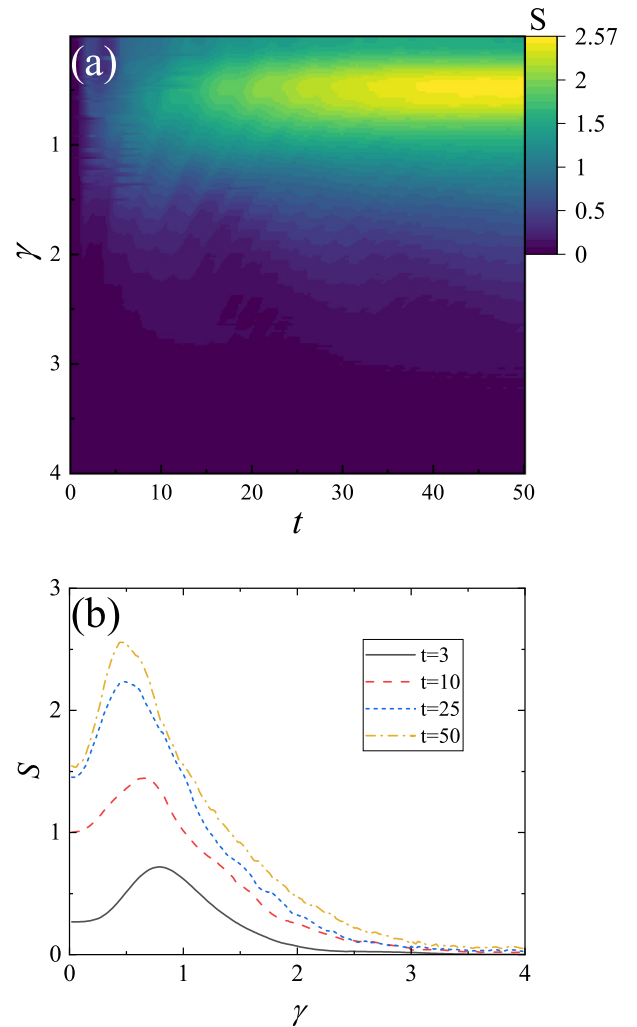


FIG. 6. Transition process of single DW. (a) The entanglement entropy  $S$  as a function of  $\gamma$  ( $0 \sim 4$ ) and time ( $0 \sim 50$ ). It is found that  $S$  grows rapidly around  $\gamma = 0.5$  and is slowed down with increasing  $\gamma$ . (b)  $S$  at  $t = 3$  (black),  $t = 10$  (red line),  $t = 25$  (blue), and  $t = 50$  (yellow), which increases at first then decreases.

Therefore, at the heterojunction between two states,  $H_+ + H_-$  results in the dissociation of DW:

$$|\dots 1001 \dots\rangle \rightarrow |\dots 0001 \dots\rangle + |\dots 1000 \dots\rangle. \quad (9)$$

Subsequently the evolution results in

$$\begin{aligned} |\dots 1000 \dots\rangle &\rightarrow |\dots 1010 \dots\rangle + \dots \\ |\dots 0001 \dots\rangle &\rightarrow |\dots 0101 \dots\rangle + \dots \\ &\dots \end{aligned} \quad (10)$$

With sufficiently long time, we can observe the diffusion of DW. Considering only the left half of the chain, for any bipartition state on sites  $i$  and  $i + 1$  ( $i \in \text{odd}$ ),  $H_+$  is inclined to turn it into  $|01\rangle$ . The periodically driven field in  $H_+$  causes a periodic phase flip. As long as the driven frequency is large enough, the left part remains in  $|10\rangle$ . A similar situation occurs for  $|\mathbb{Z}'_2\rangle$  in the right half. The crossover discussed above corresponds to the minimum frequency to trigger localization.

In consequence, the DW tends to diffuse under the PXP model and the periodic driven field holds it back, which exhibits a competitive relation depending on the driven frequency.

Different from a similar model of hard-core bosons with driven force and disorder [39], our model is in a clean system without disorder. As we know, sufficiently strong disorder always leads to the localization regime in one dimension. Therefore, in a deterministic manner, disorder-free localization should be more fascinating [40–42]. To achieve it, models such as exerting uniform force [41] or mixing two interacting hard-core particles [42] are proposed. In contrast, the modified PXP model only take into consideration the Rydberg blockade among sites stemming from intrinsic interactions. As a result, realization of localization in this system turns out to be an essential result of this work.

### C. Collision of two domain walls

We now turn to discuss the interaction and collision of two DWs, which will manifest whether they are influenced by each other while acting as information resource. To this end, we set double DWs

$$|DW_2\rangle = |10 \dots 10 : 01 \dots 010 : 01 \dots 10\rangle \quad (11)$$

at  $k = 20$  and  $k = 27$ , respectively. To avoid the nearest-neighbor Rydberg blockade, the number of sites in the second and third regions has to be odd, so two additional zeros are inserted to form the right DW. The spatial inversion symmetry still holds.

Figure 7(a) shows the  $\mathbb{Z}_2$  inhomogeneity with  $\gamma = 0$ . The diffusion of two DWs is perfectly symmetric in the spatial inversion manner. The velocity of the two DWs is also the same with that in Fig. 1. At around  $t = 13.5$ , they meet, collide, and then continue moving as before. When setting  $\gamma = 4$ , the result in Fig. 7(b) is as expected; that is, two DWs are locally static for sufficiently long time, which corresponds to the localization regime.

If regarding these diffused DWs as information carriers, the collision between them could be recognized as information communication. Intuitively, as seen in Fig. 7(a), they only pass and have no influence on each other. For the sake of demonstrating the superstability of their shape, we measure the trace distance between initial and evolving states [24,43,44]. The trace distance, quantitatively describing the closeness between two states, is defined as  $D_{\text{tr}}(\rho, \sigma) = \frac{1}{2} \|\rho - \sigma\|_1$ , where the trace norm is  $\|X\|_1 = \text{Tr} \sqrt{X^\dagger X}$ . Herein, time-dependent trace distance thus writes

$$D(t) = \frac{1}{2} \|\rho(t) - \rho(0)\|_1, \quad (12)$$

where  $\rho$  is the reduced density matrix of sites from 42 to 46 in the chain.

For a comparison, we calculate two cases, namely single DW and double DW, as shown in Fig. 8. Both of them gradually decrease as time is evolving and behave with periodic oscillations like the quantum fidelity of  $|\mathbb{Z}_2\rangle$ . Two trace distances have similar fluctuation modes with a slight difference of amplitude. Even if two DWs encounter at  $t = 13.5$ , the red line does not manifest any specific changes. This implies that two diffused DWs just solely go through each other without any effective interactions. This result is totally different from

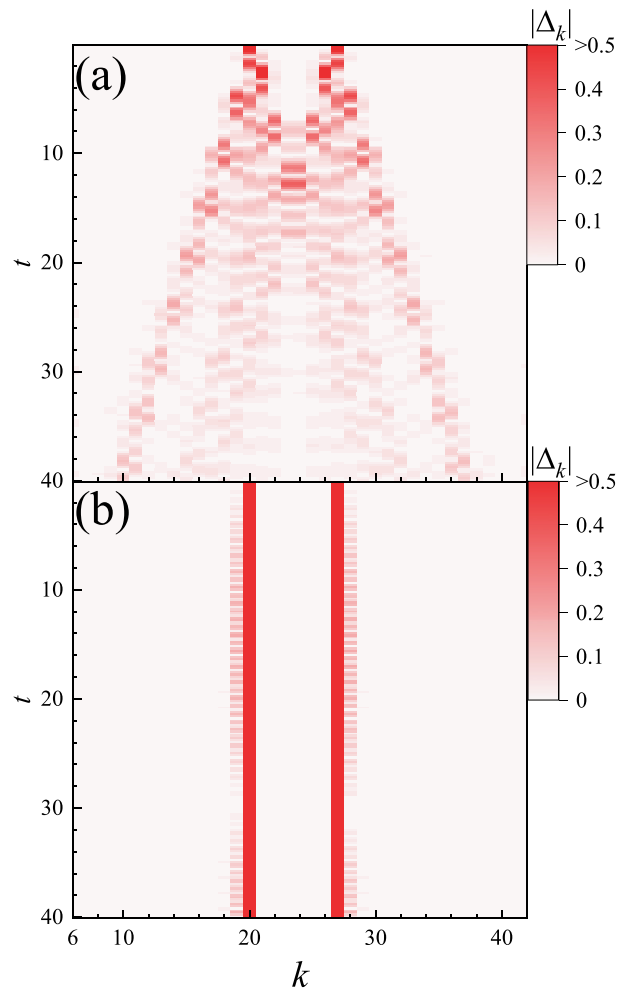


FIG. 7. The  $\mathbb{Z}_2$  inhomogeneity  $|\Delta_k|$  of double-DW system for  $t \sim 40$ . Initially, the first DW is between  $i = 40$  and  $i = 41$  and the second DW is between  $i = 53$  and  $i = 54$ . (a) For  $\gamma = 0$ , two DWs collide with each other at around  $t = 13.5$ . (b) For  $\gamma = 4$ , two DWs remain localized.

the paired soliton and antisoliton in the SSH model [45]. There is no interaction if they are far apart. When they get close, different interactions that depend on their charges emerge. Recalling the  $\Delta_{\pm}$  discussed above, the entanglement shows up between two separate parts of a single DW, while for two distinct DWs, the collision does not make a visible correlation. This result is perfectly positive, such that we can indeed regard the DWs as a resource of quantum information.

## IV. SUMMARY AND OUTLOOK

In this work, we explored the dynamics of several atypical initial states with DWs instead of normal charge density wave states. These DWs are located between  $|\mathbb{Z}_2\rangle$  and  $|\mathbb{Z}'_2\rangle$ , which spontaneously dissociate and diffuse under the PXP Hamiltonian. To observe the motion of DW, we introduce a novel quantity, i.e., the  $\mathbb{Z}_2$  inhomogeneity  $\Delta_k$ . The system with DW shows features of QMBS and the dissociation of DW leads to sufficiently long-term phase coherence and entanglement

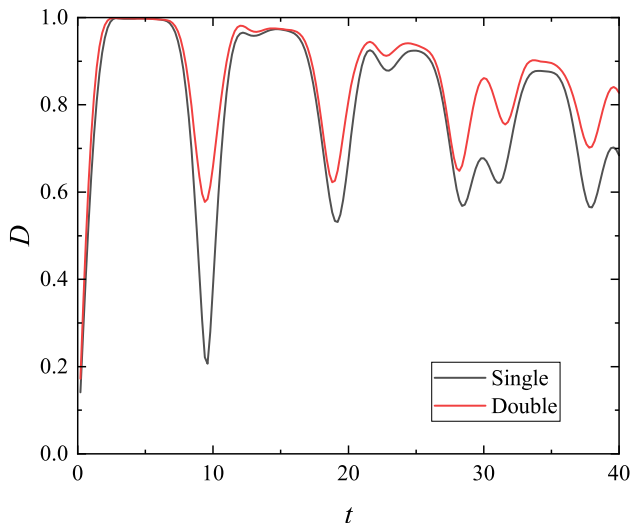


FIG. 8. The trace distance  $D(t)$  for  $t \sim 40$ , between the initial and evolving state. We focus on the collision of the two DWs so merely calculate the central 5 sites from  $i = 42$  to  $i = 46$ . For a comparison, two cases are displayed, namely the single DW (black; DW located between  $i = 40$  and  $i = 41$ ) and double DW (red; DWs are the same as in Fig. 7).

between generated DWs, suggesting they can be resources of quantum information carriers. We have also investigated the transition between prethermalization and localization. By means of FSA formulation, we construct Hamiltonian (3) with periodic driven field. This time-dependent phase difference between odd and even sites possibly hinders the diffusion of DW. High-frequency drive results in the totally disorder-free Floquet localization. Moreover, the Floquet-Magnus expansion [46] works to our system and the expansion coefficient depends on the  $\gamma$ . For one period, the first order of expansion is zero and the higher orders are composed of commutators of  $H_+$  and  $H_-$ .

It is also interesting to consider the collision and interaction of DWs. We thus set two DWs and find they have little influence on each other after collision. This further allows us to make an analogy with the propagation of information carriers. From quantum resource theories, these DW states may serve as the resource state. Whether the operation is free depends on the frequency of periodically driven field.

Throughout this work, we merely discuss the DW between  $\mathbb{Z}_2$  degenerate states. For  $\mathbb{Z}_3$  states such as  $|100\rangle$ ,  $|010\rangle$ , and  $|001\rangle$ , the research should be more interesting but more difficult, as we have to properly adapt the periodic drive and quantity of inhomogeneity for the more complicated configurations. At the very least, the DW dynamics investigated here suggest an appealing direction to study QMBS and other ETH-breaking phenomena. Preparing the Rydberg atom system with more DW configurations will be the scope of our future work.

As an additional remark, the  $|10\rangle$  and  $|01\rangle$  bipartition states remind us of the Affleck-Kennedy-Lieb-Tasaki (AKLT) spin chains [47,48]. The spin-1 AKLT model can be thought to consist of spin-1/2 Schwinger bosons. Here, if the Rydberg and ground states are regarded as  $\pm 1/2$  spin, our model can also be regarded as an extension from spin-1/2 to spin-1 [49]. The DW is therefore an interface between 1 and  $-1$  spin. In addition, QMBS in 2D Rydberg atom arrays has also been introduced [50]. Constructing DWs in the 2D PXP model refers to the DWs between different stripe phases of the 2D Hubbard model [51], which will be even more attractive subjects.

#### ACKNOWLEDGMENTS

The authors gratefully acknowledge support from the Key Research and Development Project of Guangdong Province (Grant No. 2020B0303300001), National Natural Science Foundation of China (Grant No. 11974118), and Guangdong–Hong Kong–Macao Joint Laboratory of Optoelectronic and Magnetic Functional Materials program (Grant No. 2019B121205002).

- 
- [1] M. Srednicki, *Phys. Rev. E* **50**, 888 (1994).
  - [2] L. D'Alessio, Y. Kafri, A. Polkovnikov, and M. Rigol, *Adv. Phys.* **65**, 239 (2016).
  - [3] J. M. Deutsch, *Rep. Prog. Phys.* **81**, 082001 (2018).
  - [4] E. Altman and R. Vosk, *Annu. Rev. Condens. Matter Phys.* **6**, 383 (2015).
  - [5] D. A. Abanin and Z. Papi, *Ann. Phys.* **529**, 1700169 (2017).
  - [6] D. A. Abanin, E. Altman, I. Bloch, and M. Serbyn, *Rev. Mod. Phys.* **91**, 021001 (2019).
  - [7] S. Gopalakrishnan and S. Parameswaran, *Phys. Rep.* **862**, 1 (2020).
  - [8] J. Berges, S. Borsányi, and C. Wetterich, *Phys. Rev. Lett.* **93**, 142002 (2004).
  - [9] M. Ueda, *Nat. Rev. Phys.* **2**, 669 (2020).
  - [10] H. Bernien, S. Schwartz, A. Keesling, H. Levine, A. Omran, H. Pichler, S. Choi, A. S. Zibrov, M. Endres, M. Greiner *et al.*, *Nature (London)* **551**, 579 (2017).
  - [11] C. J. Turner, A. A. Michailidis, D. A. Abanin, M. Serbyn, and Z. Papić, *Nat. Phys.* **14**, 745 (2018).
  - [12] C. J. Turner, A. A. Michailidis, D. A. Abanin, M. Serbyn, and Z. Papić, *Phys. Rev. B* **98**, 155134 (2018).
  - [13] M. Serbyn, D. A. Abanin, and Z. Papić, *Nat. Phys.* **17**, 675 (2021).
  - [14] D. Jaksch, J. I. Cirac, P. Zoller, S. L. Rolston, R. Côté, and M. D. Lukin, *Phys. Rev. Lett.* **85**, 2208 (2000).
  - [15] Z. Yao, L. Pan, S. Liu, and H. Zhai, *Phys. Rev. B* **105**, 125123 (2022).
  - [16] N. Maskara, A. A. Michailidis, W. W. Ho, D. Bluvstein, S. Choi, M. D. Lukin, and M. Serbyn, *Phys. Rev. Lett.* **127**, 090602 (2021).
  - [17] I. Mondragon-Shem, M. G. Vavilov, and I. Martin, *PRX Quantum* **2**, 030349 (2021).
  - [18] T. Iadecola and M. Schechter, *Phys. Rev. B* **101**, 024306 (2020).
  - [19] W. P. Su, J. R. Schrieffer, and A. J. Heeger, *Phys. Rev. B* **22**, 2099 (1980).



- [20] A. Fert, N. Reyren, and V. Cros, *Nat. Rev. Mater.* **2**, 17031 (2017).
- [21] A. K. Nayak, V. Kumar, T. Ma, P. Werner, E. Pippel, R. Sahoo, F. Damay, U. K. Rößler, C. Felser, and S. S. P. Parkin, *Nature (London)* **548**, 561 (2017).
- [22] G. Finocchio, F. Büttner, R. Tomasello, M. Carpentieri, and M. Kläui, *J. Phys. D* **49**, 423001 (2016).
- [23] V. Emery, S. Kivelson, and J. Tranquada, *Proc. Natl. Acad. Sci. U.S.A.* **96**, 8814 (1999).
- [24] E. Chitambar and G. Gour, *Rev. Mod. Phys.* **91**, 025001 (2019).
- [25] M. Lostaglio, *Rep. Prog. Phys.* **82**, 114001 (2019).
- [26] F. M. Surace, P. P. Mazza, G. Giudici, A. Lerose, A. Gambassi, and M. Dalmonte, *Phys. Rev. X* **10**, 021041 (2020).
- [27] J. P. Garrahan, *Physica A* **504**, 130 (2018).
- [28] K. Sacha and J. Zakrzewski, *Rep. Prog. Phys.* **81**, 016401 (2018).
- [29] D. V. Else, C. Monroe, C. Nayak, and N. Y. Yao, *Annu. Rev. Condens. Matter Phys.* **11**, 467 (2020).
- [30] Y. Ono and A. Terai, *J. Phys. Soc. Jpn.* **59**, 2893 (1990).
- [31] G. Vidal, *Phys. Rev. Lett.* **98**, 070201 (2007).
- [32] M. Fishman, S. R. White, and E. M. Stoudenmire, [arXiv:2007.14822](https://arxiv.org/abs/2007.14822).
- [33] E. Hagley, X. Maître, G. Nogues, C. Wunderlich, M. Brune, J. M. Raimond, and S. Haroche, *Phys. Rev. Lett.* **79**, 1 (1997).
- [34] I. Marvian and R. W. Spekkens, *Nat. Commun.* **5**, 3821 (2014).
- [35] I. Marvian and R. W. Spekkens, *Phys. Rev. A* **90**, 062110 (2014).
- [36] M. Žnidarič, T. Prosen, and P. Prelovšek, *Phys. Rev. B* **77**, 064426 (2008).
- [37] R. Fan, P. Zhang, H. Shen, and H. Zhai, *Sci. Bull.* **62**, 707 (2017).
- [38] D.-L. Deng, X. Li, J. H. Pixley, Y.-L. Wu, and S. Das Sarma, *Phys. Rev. B* **95**, 024202 (2017).
- [39] E. Bairey, G. Refael, and N. H. Lindner, *Phys. Rev. B* **96**, 020201(R) (2017).
- [40] A. Smith, J. Knolle, D. L. Kovrizhin, and R. Moessner, *Phys. Rev. Lett.* **118**, 266601 (2017).
- [41] E. van Nieuwenburg, Y. Baum, and G. Refael, *Proc. Natl. Acad. Sci. U.S.A.* **116**, 9269 (2019).
- [42] M. Schiulaz, A. Silva, and M. Müller, *Phys. Rev. B* **91**, 184202 (2015).
- [43] C. Fuchs and J. van de Graaf, *IEEE Trans. Inf. Theory* **45**, 1216 (1999).
- [44] B. Aaronson, R. L. Franco, G. Compagno, and G. Adesso, *New J. Phys.* **15**, 093022 (2013).
- [45] H. Zhao, Y. Chen, Y. Yan, Z. An, and C. Wu, *Europhys. Lett.* **100**, 57005 (2012).
- [46] M. Bukov, L. D'Alessio, and A. Polkovnikov, *Adv. Phys.* **64**, 139 (2015).
- [47] S. Moudgalya, S. Rachel, B. A. Bernevig, and N. Regnault, *Phys. Rev. B* **98**, 235155 (2018).
- [48] S. Moudgalya, N. Regnault, and B. A. Bernevig, *Phys. Rev. B* **98**, 235156 (2018).
- [49] N. Shiraiishi, *J. Stat. Mech.: Theory Exp.* (2019) 083103.
- [50] C.-J. Lin, V. Calvera, and T. H. Hsieh, *Phys. Rev. B* **101**, 220304(R) (2020).
- [51] M. Raczkowski, R. Frésard, and A. M. Oleś, *Phys. Rev. B* **73**, 174525 (2006).